Joint Video Packet Scheduling, Subchannel Assignment and Power Allocation for Cognitive Heterogeneous Networks

Lei Xu, *Member, IEEE,* Arumugam Nallanathan, *Fellow, IEEE,* and Xiaoqin Song

Abstract—In this paper, a joint video scheduling, subchannel assignment, and power allocation problem in cognitive heterogeneous networks are modeled as a mixed integer non-linear programming (MINLP), which maximizes the minimum video transmission quality among different secondary mobile terminals (MTs) subject to the total available energy at each secondary, the total interference power at each primary base station, the total available capacity at each radio interface of each secondary MTs, and the video sequence encoding characteristic. In order to solve it, we decompose the original MINLP as joint subchannel and power allocation problem and video packet scheduling problem. Then, we model the joint subchannel and power allocation problem as a max–min fractional programming, and transform it as a convex optimization problem. Finally, we utilize dual decomposition method to design a joint subchannel and power allocation algorithm, and propose a video packet scheduling scheme based on auction theory to maximize the video quality for each secondary MT. Simulation results demonstrate that the proposed framework not only improves the video transmission quality significantly, but also guarantees the fairness among different secondary MTs.

Index Terms—Cognitive heterogeneous networks, packet scheduling, video traffic, auction theory, mixed integer non-linear programming.

I. Introduction

WIRELESS communication medium becomes heterogeneous environment with various wireless networks [1]–[4]. Heterogeneous wireless networks received broad attention from mobile network operators [5]. However, the spectrum resources at wireless networks cannot be utilized efficiently. Specially, spectrum is not fully utilized when the traffic in the cell is light. In order to enhance the spectrum efficiency further, cognitive radio technology can be

applied into heterogeneous wireless networks via accessing the licensed spectrum opportunistically. Many international standardization organization have drafted several standards, e.g., 802.11 af, 802.19 TG 1, IEEE 802.22, and LTE-U to utilize cognitive radio technology [6]. In cognitive heterogeneous networks, secondary MT can utilize multi radio interfaces to communicate with different secondary base stations (BSs) simultaneously. In one typical application scenario, cognitive macrocell can provide wireless backhaul to secondary MTs with low-to-medium service, while cognitive microcell can provide high-rate service to secondary MTs. In the future wireless networks, video traffic is one of the most popular mobile services [7]. The international companies, like Cisco, predict that video services will be in the range of 80 to 90 percent of global consumer traffic by 2018 [8]. Since MTs are resource-constrained compared to the desktop equivalents, it is a resource hungry application. Hence, it is a challenging task to provide a good video quality.

In cognitive wireless network, the resource management algorithms for video traffic can be classified into three categories based on different layers, e.g. the call admission control problem at the network layer [9], the packet schedule problems at the link layer [10], [11] and the joint bandwidth and power allocation problems at the physical layer [12]–[15]. In [9], a statistical call admission control scheme for video traffic is proposed for cognitive wireless network. For the packet scheduling, a dynamic channel selection scheme, based on priority packet scheduling, for cognitive wireless network is proposed to transmit the delay-sensitive video packets over wireless fading channel [10]. In [11], a statistic traffic control scheme, incorporated the packet transmission scheduling with the admission control, for cognitive wireless network is designed to guarantee the packet-level quality of service (QoS) requirements. Except for the packet scheduling problems for cognitive wireless network, video packet scheduling algorithms for ad hoc networks have been studied in recent years, e.g., [16], [17]. In [16], the performance of video streaming over mobile ad hoc networks from the perspective of energy-efficiency and spectrum-efficiency is analyzed. Additionally, the delayed control channels for distributed wireless video scheduling is quantifying [17].

For joint bandwidth and power allocation, an optimal joint subcarrier and power allocation scheme is proposed for orthogonal frequency division multiple access (OFDMA)-based cognitive wireless networks, subject to minimum secondary receiver video quality and primary receiver interference

L. Xu is with the School of Computer Science and Engineering, Nanjing University of Science and Technology, Nanjing 210094, China (e-mail: xulei_marcus@126.com).

A. Nallanathan is with the Department of Informatics, King's College London, London WC2R 2LS, U.K. (e-mail: nallanathan@ieee.org).

X. Song is with the College of Electronic and Information Engineering, Nanjing University of Aeronautics and Astronautics, Nanjing 210096, China (e-mail: xiaoqin.song@163.com).

threshold [12]. In [13], the source rate, the transmission rate and the transmission power at each video session are jointly optimized for cognitive wireless network to provide bit-level QoS of the video streaming sessions. Based on [13], the resource allocation problem of multi-layered video streaming for multi-channel cognitive wireless networks is investigated [14]. In [15], the optimization problem for video streaming in cognitive femtocell network is formulated, and a resource allocation framework capturing the key design issues is developed via a stochastic programming theory. In [18], a novel channel allocation technique to overcome this limitation for cognitive wireless network based on utilizing several non-contiguous channels is proposed.

There are some resource allocation algorithms for cognitive heterogeneous networks [19]–[21]. For OFDMA-based cognitive heterogeneous networks, a joint subcarrier and antenna state selection via reconfigurable antennas is proposed [19]. For OFDM-based heterogeneous cognitive radio networks, a joint subcarrier and power allocation based on imperfect spectrum sensing is investigated with the total transmission power constraint, interference constraint and QoS constraint to maximize the capacity [20]. An energy-efficient resource allocation problem in heterogeneous cognitive radio networks with femtocells is formulated with the Stackelberg game and a gradient based iteration algorithm is proposed to obtain the Stackelberg equilibrium solution [21].

Although the packet scheduling problems for cognitive wireless network are investigated in [10] and [11], how video traffic affects the joint subchannel and power allocation and packet scheduling for cognitive heterogeneous networks utilizing the multi-homing technology needs further studies. In this paper, we study the joint video packet scheduling, subchannel assignment, and power allocation for cognitive heterogeneous networks. The contributions of this work is summarized as follows: (i) We formulate an uplink video packet scheduling problem as max-min fractional MINLP to jointly allocate video packet at the link layer, subchannel and power at the physical layer among different secondary MTs and among different radio interfaces for each secondary MT; (ii) We divide the uplink video packet scheduling into two subproblems, i.e., joint subchannel and power allocation subproblem and video packet scheduling subproblem; (iii) We utilize the dual decomposition method to design the optimal subchannel and power allocation algorithm, and propose a heuristic packet scheduling scheme with the auction theory. Simulation results demonstrate proposed algorithms improve the video quality effectively, and strike a balance between fairness and video quality.

The rest of this paper is organized as follows. The system model is described in Sections II. Section III presents the problem formulation. An optimal subchannel and power allocation scheme and a content-aware video scheduling framework are given in Section IV. Finally, performance evaluation and conclusions are given in Sections V and VI, respectively.

II. SYSTEM MODEL

In this section, the system model and power consumed model are described firstly. Then, the transmission rate model
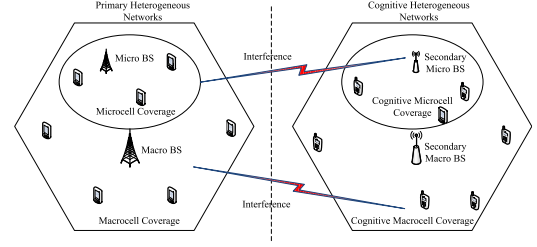

Fig. 1. Cognitive heterogeneous networks.

and interference power model are presented. Finally, video traffic model is introduced.

A. System Description

In this paper, there is a set, $N = \{1, 2, \cdots, N\}$, of wireless networks, operated by different operators. In each wireless network, we adopt the central control model to manage the wireless network unlike the random access network [22]. Additionally, there exists a set, $\mathcal{S}_n = \{1, 2, \cdots, S_n\}$, of secondary BSs, and a set, $\mathcal{S}_n^* = \{1, 2, \cdots, S_n\}$, of primary BSs[1] Since the coverage of secondary BSs for each wireless network is different from each other, the geographical region is partitioned into multiple service areas, as shown in Fig. 1. In the geographical region, there exists a set, $\mathcal{M} = \{1, 2, \cdots, M\}$, of secondary MTs, and a subset of secondary MTs, $\mathcal{M}_{ns} = \{1, 2, \cdots, M_{ns}\} \in \mathcal{M}$, lie in the coverage area of cognitive network n BS s. In each primary wireless network, the bandwidth is divided into several orthogonal subchannels, and orthogonal frequency division multiplexing (OFDM) technology is adopted. In cognitive network n BS s, the sensed available subchannel set is $\mathcal{K}_{ns}^v = \{1, 2, \cdots, K_{ns}^v\}$. In the same cognitive network, interference mitigation is achieved by interference management schemes[2] e.g., [25], [26], and the interference power at primary BS should be controlled according to the interference temperature model [27]. With multi-homing mechanism and multiple radio interfaces at each secondary MT, each secondary MT can communicate with multiple secondary BSs, simultaneously.

B. Power Consumption Model

The consumed power at each interface for each secondary MT includes three parts. The first part is a fixed circuit power for each interface at each secondary MT given by Q_{nsm}^F. The second part is a dynamic part referring to the digital circuit consumed power, and the third part scales with the allocated bandwidth. The dynamic consumed power, Q_{nsm}^D, for each interface at each secondary MT is [28]

$$Q_{nsm}^D = Q_D^{\text{ref}} + \sigma_{nsm} \frac{\sum\limits_{k \in \mathcal{K}_{ns}} \rho_{nsm}^k B_{ns}}{B_{\text{ref}}} \qquad (1)$$

[1]The number of primary BSs and the number of secondary BSs can be different. For the convenience of analysis, we assume the number of primary BSs and the number of secondary BSs are equal in this work and this is the special case.

[2]In this work, we assume the inter-cell interference in the same cognitive network can be mitigated via the interference management schemes, and this can help us to simplify the problem [23], [24]. Therefore, we only consider the signal to noise ratio (SNR) instead of the signal to interference and noise ratio (SINR). The results of this work can be easily extended to consider the inter-cell interference, i.e., SINR.

where ρ_{nsm}^k is the subchannel allocation indicator variable for cognitive network n BS s MT m over the kth subchannel, B_{ns} denotes the subchannel bandwidth for cognitive network n BS s, Q_D^{ref} is the digital circuit power consumption for a reference bandwidth B_{ref}. σ_{nsm} is a proportional constant. Denote $Q_{nsm} = Q_{nsm}^F + Q_D^{\text{ref}}$ and $\zeta_{nsm} = \sigma_{nsm}/B_{\text{ref}}$.

Consequently, the total power for each interface at each secondary MT is [23]

$$P_{nsm}^{\text{T}} = \frac{\sum\limits_{k \in \mathcal{K}_{as}} P_{nsm}^k}{\eta_{nsm}} + Q_{nsm} + \zeta_{nsm} \sum\limits_{k \in \mathcal{K}_{as}} \rho_{nsm}^k B_{ns} \quad (2)$$

where η_{nsm} denotes the power amplifier coefficient for cognitive network n BS s to communicate with MT m. For $m \notin M_{ns}$, $P_{nsm}^k = Q_{nsm}^F = Q_{nsm}^D = 0$.

C. Transmission Rate Model

The transmission rate, R_{nsm}^k, for cognitive network n BS s MT m over subchannel k is

$$R_{nsm}^k = B_{ns} \log_2 \left(1 + \frac{P_{nsm}^k g_{nsm}^k}{B_{ns} n_0 + I_{nsk}^{\text{cross}}} \right), \quad k \in \mathcal{K}_{as}. \quad (3)$$

where I_{nsk}^{cross} is the cross channel interference at the kth subchannel introduced to secondary MT from primary network n BS s, g_{nsm}^k is the channel power gain over subchannel k from MT m to cognitive network n BS s, and n_0 is one-sided noise power spectral density.

D. Interference Power Model

The nominal spectrum of the jth subchannel spans from $f_s + (k-1)B_{ns}$ to $f_s + kB_{ns}$, where f_s is the starting frequency. When the secondary MT transmits data over the kth subchannel with unit transmission power, the interference, I_{nsm}^{kj}, introduced to the jth subchannel of primary network n BS s from the kth subchannel of cognitive network n BS s MT m is [29] and [30]

$$I_{nsm}^{kj} = \int_{(j-1)B_{ns}-(k-0.5)B_{ns}}^{jB_{ns}-(k-0.5)B_{ns}} h_{nsm}^k \varphi(f) df \quad (4)$$

where h_{nsm}^k is the channel power gain over subchannel k from cognitive network n BS s MT m to primary network n BS s, and $\varphi(f)$ is the power spectrum density of OFDM signal.

$$\varphi(f) = T \left(\frac{\sin \pi f T}{\pi f T} \right)^2 \quad (5)$$

where T is OFDM symbol duration.

E. Video Traffic Model

Consider a video traffic at each secondary MT. There are a base layer and several enhancement layers in the video layered sequence. Time is divided into time slots, $\mathcal{T} = \{1, 2, \cdots, T\}$, which is with equal duration, τ. The number of time slots, T, is estimated according to video call duration. From each layer, the secondary MT has a new group of picture (GoP) for each transmission τ [24], and this model can be applied to a general one, e.g., H.264/MPEG-4 [31]–[33]. From different layers, each time slot includes a set of frames, $\mathcal{F} = \{1, 2, \cdots, F\}$. Frame types is divided into B, I, or P types. Each frame
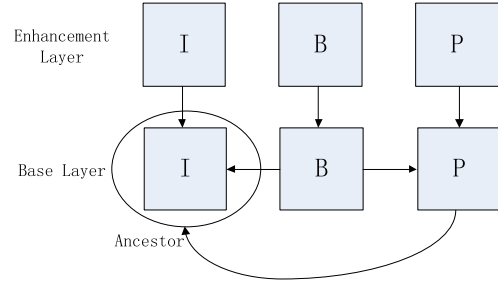

Fig. 2. GoP structure with frame dependencies [3].

contains many packets. Frame f is divided into L_f packets, $\mathcal{L}_f = \{1, 2, \cdots, L_f\}$, and each packet has h_f bits. Since some frames are encoded based on the prediction of other frames, dependencies exist in these frames. Consequently, decoding video packets in one frame depends on successfully decoding packets from other frames. Hence, a set of ancestors, $\mathcal{A}_l^f$, exists for each packet, l_f. Video packets in A_l^f have smaller delay deadline and higher distortion impact than packet l_f [3]. These dependencies among packets of different frames, within one time slot, are expressed using a directed acyclic graph, as shown in Figure 2. In Fig. 2, the circled I frame is an ancestor for the first B and P frames in the base layer and the I frame in the enhancement layer [3].

Since the path losses for the different interfaces at each secondary MT to different secondary BSs are different, the transmission capacities for the different interfaces at each secondary MT are different. In this work, we do not consider the transmission delay at each interface for each secondary MT like other video packet scheduling works. We only consider the playback delay about video traffic [34]. $\Delta D = |d_{f+1} - d_f|$ is the delay deadline difference for any two consecutive frames, where d_f is the delay deadline for frame f. Via the video packet scheduling algorithm, we assign the less video packets to the interface with the less transmission capacity. If the interface at the secondary MT cannot satisfy the transmission rate of the assigned video packets, the new assigned video packets are dropped. The losses of the video packet at the different interfaces lead to the reduction of the video quality. This is evaluated by the simulation about the video quality based on the proposed joint subchannel assignment, power allocation and video packet scheduling algorithm.

III. PROBLEM FORMULATION

In cognitive heterogeneous networks, secondary MTs cooperate in resource allocation to achieve the better performance. At the beginning of each time slot, a joint subchannel and power allocation decision, i.e., ρ_{nsm}^k and P_{nsm}^k, is made for cognitive network n BS s MT m at subcarrier k, and a video packet scheduling decision, x_{nsm}^{fl}, is designed, where $x_{nsm}^{fl} = 1$ represents frame f video packet l is assigned to cognitive network n BS s MT m; otherwise, $x_{nsm}^{fl} = 0$. The video packet transmission decision policy, on ρ_{nsm}^k, P_{nsm}^k and x_{nsm}^{fl}, are designed based on the video characteristics, available radio resources at different radio interfaces and at different secondary MTs, and secondary MT battery energy limitation. Additionally, the channel gains remain constant at one time slot, and are different from one time slot to another.

The subchannel allocation, ρ_{nsm}^k, should satisfy

$$\sum_{m \in \mathcal{M}_{ns}} \rho_{nsm}^k \leq 1 \qquad (6)$$

where $\rho_{nsm}^k \in [0,1]$ is the fraction of the kth subchannel allocated to cognitive network n BS s MT m.

The total power consumption, $P_m = \sum_{n \in \mathcal{N}} \sum_{s \in \mathcal{S}_n} P_{nsm}^T$, for MT m should satisfy the maximum available energy, i.e.,

$$P_m \leq \frac{E_m}{\tau} \qquad (7)$$

where E_m is the energy budget per time slot for MT m.

The total interference power at primary network n BS s does not exceed the maximum interference threshold, I_{ns}^{th}, for primary network n BS s, i.e.,

$$\sum_{m \in \mathcal{M}_{ns}^c} \sum_{k \in \mathcal{K}_{ns}^v} C_{nsm}^k I_{nsm}^k \leq I_{ns}^{\text{th}} \qquad (8)$$

where $I_{nsm}^k = \sum_{j \neq k, j \in \mathcal{K}_{ns}^v} I_{nsm}^{kj}$ is the interference power for cognitive network n BS s MT m on the kth subchannel, and $C_{nsm}^k = \rho_{nsm}^k P_{nsm}^k$ is the actual power consumption for cognitive network n BS s MT m over the kth subchannel at a time frame interval. Additionally, the interference temperature model is widely adopted in the resource allocation at cognitive radio networks, and it is proved to be simple and effective, e.g., [29], [30]. Hence, we adopt it to describe the interference impact of the secondary MTs from cognitive heterogeneous networks to the primary BSs at primary heterogeneous networks.

The overall transmission rate for video packet transmission over a given interface needs to satisfy the achieved transmission rate over it, i.e.,

$$\sum_{f \in \mathcal{F}} \sum_{l_f \in \mathcal{L}_f} x_{nsm}^{fl} r(l_f) \leq \sum_{k \in \mathcal{K}_{us}} R_{nsm}^k \qquad (9)$$

where $r(l_f) = h_f / \Delta D$ is the minimum transmission rate for a video packet, $l_f \in \mathcal{L}_f$, and $\Delta D = |d_{f+1} - d_f|$ is the delay deadline difference for any two consecutive frames, where d_f is the delay deadline for frame f.

Since the ancestors of video packets are not scheduled for transmission, they should not be transmitted. Consequently, video packet scheduling should capture the dependence relationship among different packets, i.e.,

$$x_{nsm}^{fl} \leq x_{nsm}^{f^* l^*}, \quad \forall l_{f^*}^* \in A_l^f, \ l_f \in \mathcal{L}_f, \ f \in \mathcal{F} \qquad (10)$$

where $x_{nsm}^{f^* l^*}$ represents frame f^* packet l^* is allocated to cognitive network n BS s MT m.

Additionally, a video packet can be assigned to at most one interface, i.e.,

$$\sum_{n \in \mathcal{N}} \sum_{s \in \mathcal{S}_n} x_{nsm}^{fl} \leq 1. \qquad (11)$$

The optimization framework maximizes the minimization of the perceived video quality, and the video quality is defined as

$$V_m = \sum_{n \in \mathcal{N}} \sum_{s \in \mathcal{S}_n} \sum_{f \in \mathcal{F}} \sum_{l_f \in \mathcal{L}_f} v_f^l x_{nsm}^{fl} \qquad (12)$$

where v_f^l characterizes the video distortion impact of a packet l_f in frame f. Since the video information has the non-stationary nature, all the video packets are not equivalent valuable, and we get the video distortion impact values from [34].

Consequently, the uplink video packet scheduling problem is formulated as

$$OP1: \max_{\rho_{nsm}^k, C_{nsm}^k} \{\min V_m\}$$
$$s.t. \ (6) - (11), \rho_{nsm}^k \geq 0, C_{nsm}^k \geq 0, x_{nsm}^{fl} \in \{0, 1\}$$
$$(13)$$

where problem (13) is a max-min MINLP.

IV. JOINT VIDEO PACKET SCHEDULING, SUBCHANNEL ASSIGNMENT AND POWER ALLOCATION

Intuitively, video transmission quality is maximized, when more video packets are transmitted. Since problem (10) involves real variables (ρ_{nsm}^k, C_{nsm}^k) and binary variables x_{nsm}^{fl}, it is a max-min MINLP. Additionally, it is NP-hard problem. Consequently, we decouple problem (13) into two sub-problems, i.e., joint subchannel and power allocation problem and video packet scheduling problem[3] The first sub-problem finds the allocated subchannel and transmission power for each interface and each secondary MT maximizing the achieved data rate, subject to the secondary MT battery energy limitation, the interference power limitation, and the available capacity at each radio interface. The second sub-problem schedules the most valuable video packets among different interfaces for each secondary MT, given the transmission power and the available subchannel.

A. Joint Subchannel and Power Allocation

Although problem (13) maximizes the minimum video quality among different secondary MTs, it can not guide the subchannel and power allocation directly. Consequently, the normalized video transmission quality, $R_m \sum_{f \in \mathcal{F}} \sum_{l_f \in \mathcal{L}_f} v_f^l / \sum_{f \in \mathcal{F}} \sum_{l_f \in \mathcal{L}_f} r(l_f)$, is defined. Additionally, the subchannel and power allocation strategy adjusts based on the channel condition, to maximize the minimum video quality among different secondary MTs, while satisfying the secondary MT battery energy limitation, the available vacant subchannel resources, and the total interference power limitation, i.e.,

$$OP2: \max_{\rho_{nsm}^k, C_{nsm}^k} \left\{ \min : \frac{\sum_{f \in \mathcal{F}} \sum_{l_f \in \mathcal{L}_f} v_f^l}{\sum_{f \in \mathcal{F}} \sum_{l_f \in \mathcal{L}_f} r(l_f)} R_m \right\}$$
$$s.t. \ (6) - (8), \ \rho_{nsm}^k \geq 0, \ C_{nsm}^k \geq 0 \qquad (14)$$

where $R_m = \sum_{n \in \mathcal{N}} \sum_{s \in \mathcal{S}_n} \sum_{k \in \mathcal{K}_{us}^v} \rho_{nsm}^k R_{nsm}^k$ is the total transmission rate for secondary MT m.

---

[3]Since the above max-min MINLP is a NP-hard problem, we can not obtain the optimal resource allocation solution. Usually, the MINLP is decomposed with the subproblem with integer variables and the subproblem with the real variables to reduce the computational complexity. Additionally, this decomposition method is proved to be effective, e.g., [3], [35].

Consequently, problem (14) can be rewritten as

$$OP3: \max_{\rho_{nsm}^k, C_{nsm}^k} \vartheta$$

$$S.t.: \frac{\sum\limits_{f\in\mathcal{F}}\sum\limits_{l_f\in\mathcal{L}_f} v_f^l}{\sum\limits_{f\in\mathcal{F}}\sum\limits_{l_f\in\mathcal{L}_f} r\left(l_f\right)} R_m \geq \vartheta, \ \forall m$$

$$(6)-(8), \ \rho_{nsm}^k \geq 0, \ C_{nsm}^k \geq 0, \ \vartheta \geq 0 \tag{15}$$

where $\vartheta = \min\limits_{m\in\mathcal{M}} : R_m \sum\limits_{f\in\mathcal{F}}\sum\limits_{l_f\in\mathcal{L}_f} v_f^l \Big/ \sum\limits_{f\in\mathcal{F}}\sum\limits_{l_f\in\mathcal{L}_f} r\left(l_f\right)$.

Then, the objective function in problem (15) is transformed into a twice differentiable function, $U(\vartheta) = \log_2(1 + \vartheta)$, by a preparatory procedure and the equivalent transformation form is

$$OP4: \max_{\rho_{nsm}^k, C_{nsm}^k} U(\vartheta)$$

$$S.t.: \frac{\sum\limits_{f\in\mathcal{F}}\sum\limits_{l_f\in\mathcal{L}_f} v_f^l}{\sum\limits_{f\in\mathcal{F}}\sum\limits_{l_f\in\mathcal{L}_f} r\left(l_f\right)} R_m \geq \vartheta, \ \forall m$$

$$(6)-(8), \ \rho_{nsm}^k \geq 0, \ C_{nsm}^k \geq 0, \ \vartheta \geq 0 \tag{16}$$

where $U(\vartheta)$ is a monotone increasing function, and $U(\vartheta) = \log_2(1 + \vartheta)$ is adopted to guarantee the equivalence of problem (15) and problem (16).

Proposition 1: Problem (16) is a convex optimization problem.

Proof: see appendix A.

Since problem (16) is a convex programming, a strong duality exists, and the optimal values for the primal and dual problems are equal. Consequently, it is appropriate to solve it with the dual decomposition method.

The Lagrangian function for problem (16) is

$$L\left(\vartheta, \alpha_m, \beta_m, u_{nsk}, v_{ns}, \rho_{nsm}^k, C_{nsm}^k\right)$$
$$= \log_2(1+\vartheta)$$
$$+ \sum_{n\in\mathcal{N}}\sum_{s\in\mathcal{S}_n} v_{ns}\left(I_{ns}^{\text{th}} - \sum_{m\in\mathcal{M}}\sum_{k\in\mathcal{K}_{ns}^v} C_{nsm}^k I_{nsm}^k\right)$$
$$+ \sum_{n\in\mathcal{N}}\sum_{s\in\mathcal{S}_n}\sum_{k\in\mathcal{K}_{ns}^v} u_{nsk}\left(1 - \sum_{m\in\mathcal{M}} \rho_{nsm}^k\right)$$
$$+ \sum_{m\in\mathcal{M}} \alpha_m\left(\frac{\sum\limits_{f\in\mathcal{F}}\sum\limits_{l_f\in\mathcal{L}_f} v_f^l}{\sum\limits_{f\in\mathcal{F}}\sum\limits_{l_f\in\mathcal{L}_f} r\left(l_f\right)} R_m - \vartheta\right)$$
$$+ \sum_{m\in\mathcal{M}} \beta_m\left(\frac{E_m}{\tau} - P_m\right) \tag{17}$$

where α_m is a Lagrangian multiplier for the first constraint condition, β_m, u_{nsk}, and v_{ns} are Lagrangian multipliers for constraints (6)-(8), respectively.

According to (17), the dual function, $h(\alpha_m, \beta_m, u_{nsk}, v_{ns})$, is

$$h(\alpha_m, \beta_m, u_{nsk}, v_{ns})$$
$$= \begin{cases} \min\limits_{\rho_{nsm}^k, C_{nsm}^k} \ L\left(\alpha_m, \beta_m, u_{nsk}, v_{ns}, \rho_{nsm}^k, C_{nsm}^k\right) \\ S.t.: \ \rho_{nsm}^k \geq 0, C_{nsm}^k \geq 0. \end{cases} \tag{18}$$

Additionally, the dual problem is

$$OP5: \max_{\substack{\alpha_m, \beta_m \\ u_{nsk}, v_{ns}}} h(\alpha_m, \beta_m, u_{nsk}, v_{ns})$$

$$S.t.: \ \alpha_m \geq 0, \beta_m \geq 0, u_{nsk} \geq 0, v_{ns} \geq 0. \tag{19}$$

Problem (19) can be simplified to

$$L_m = \alpha_m R_m \frac{\sum\limits_{f\in\mathcal{F}}\sum\limits_{l_f\in\mathcal{L}_f} v_f^l}{\sum\limits_{f\in\mathcal{F}}\sum\limits_{l_f\in\mathcal{L}_f} r\left(l_f\right)} - u_{nsk} \sum_{m\in\mathcal{M}} \rho_{nsm}^k$$
$$- \beta_m P_m - v_{ns} \sum_{m\in\mathcal{M}}\sum_{k\in\mathcal{K}_{ns}^v} C_{nsm}^k I_{nsm}^k. \tag{20}$$

Consequently, each secondary MT can solve its own utility maximization, i.e.,

$$OP6: \max L_m$$
$$S.t.: \ \rho_{nsm}^k \geq 0, C_{nsm}^k \geq 0. \tag{21}$$

Given C_{nsm}^k, α_m, β_m, u_{nsk} and v_{ns}, the optimal subchannel allocation, ρ_{nsm}^k, can be calculated with (22) by applying KKT condition on (21).

$$\frac{\partial L_m}{\partial \rho_{nsm}^k} = 0. \tag{22}$$

From (22), we can obtain

$$\alpha_m \frac{\sum\limits_{f\in\mathcal{F}}\sum\limits_{l_f\in\mathcal{L}_f} v_f^l}{\sum\limits_{f\in\mathcal{F}}\sum\limits_{l_f\in\mathcal{L}_f} r\left(l_f\right)} \frac{\partial R_m}{\partial \rho_{nsm}^k} - \beta_m \frac{\partial P_m}{\partial \rho_{nsm}^k} - \mu_{nsk} = 0 \tag{23}$$

$$\frac{\partial R_m}{\partial \rho_{nsm}^k} = R_{nsm}^k - \frac{B_{ns} C_{nsm}^k g_{nsm}^k}{W_{nsm}^k \ln 2} \tag{24}$$

$$\frac{\partial P_m}{\partial \rho_{nsm}^k} = B_{ns}\zeta_{nsm} - \frac{C_{nsm}^k}{\left(\rho_{nsm}^k\right)^2 \eta_{nsm}} \tag{25}$$

and

$$W_{nsm}^k = \rho_{nsm}^k\left(B_{ns} n_0 + I_{nsm}^{cross}\right) + C_{nsm}^k g_{nsm}^k. \tag{26}$$

Using the Newtons method on (23)-(26), the optimal subchannel solution is

$$\rho_{nsm}^k = \left[g_\rho\left(C_{nsm}^k, \alpha_m, \beta_m, u_{nsk}, v_{ns}\right)\right]^+ \tag{27}$$

where $[\bullet]^+$ is a projection on the positive orthant to account for ρ_{nsm}^k.

Given ρ_{nsm}^k, α_m, β_m, u_{nsk} and v_{ns}, the optimal actual power, C_{nsm}^k, can be calculated with (28) by applying KKT condition on (21).

$$\frac{\partial L_m}{\partial C_{nsm}^k} = 0. \tag{28}$$

From (28), we can obtain

$$\alpha_m \frac{\sum_{f \in \mathcal{F}} \sum_{l_f \in \mathcal{L}_f} v_f^l}{\sum_{f \in \mathcal{F}} \sum_{l_f \in \mathcal{L}_f} r(l_f)} \frac{\partial R_m}{\partial C_{nsm}^k} - \beta_m \frac{\partial P_m}{\partial C_{nsm}^k} - v_{ns} I_{nsm}^k = 0 \quad (29)$$

$$\frac{\partial R_m}{\partial C_{nsm}^k} = \frac{\rho_{nsm}^k g_{nsm}^k B_{ns}}{\left[\rho_{nsm}^k \left(B_{ns} n_0 + I_{nsk}^{\text{cross}} \right) + C_{nsm}^k g_{nsm}^k \right] \ln 2} \quad (30)$$

and

$$\frac{\partial P_m}{\partial C_{nsm}^k} = \frac{1}{\rho_{nsm}^k \eta_{nsm}}. \quad (31)$$

Using the Newtons method on (29)-(31), the optimal actual power, C_{nsm}^k, is

$$C_{nsm}^k = \left[g_C \left(\rho_{nsm}^k, \alpha_m, \beta_m, u_{nsk}, v_{ns} \right) \right]^+. \quad (32)$$

For a fixed ρ_{nsm}^k and C_{nsm}^k, a gradient descent method can be applied to calculate the optimal values for α_m, β_m, u_{nsk}, and v_{ns}, i.e.,

$$\alpha_m (i+1) = [\alpha_m (i) + \Delta \varepsilon_1 \alpha_1]^+ \quad (33)$$

$$\beta_m (i+1) = \left[\beta_m (i) + \Delta \varepsilon_2 \left(\frac{E_m}{\tau} - P_m \right) \right]^+ \quad (34)$$

$$u_{nsk} (i+1) = \left[u_{nsk} (i) + \Delta \varepsilon_3 \left(1 - \sum_{m \in \mathcal{M}} \rho_{nsm}^k \right) \right]^+ \quad (35)$$

$$v_{ns} (i+1) = [v_{ns} (i) + \Delta \varepsilon_4 v_1]^+ \quad (36)$$

$$\alpha_1 = \frac{\sum_{f \in \mathcal{F}} \sum_{l_f \in \mathcal{L}_f} v_f^l}{\sum_{f \in \mathcal{F}} \sum_{l_f \in \mathcal{L}_f} r(l_f)} R_m - \vartheta \quad (37)$$

and

$$v_1 = I_{ns}^{\text{th}} - \sum_{m \in \mathcal{M}} \sum_{k \in \mathcal{K}_{ns}^v} C_{nsm}^k I_{nsm}^k \quad (38)$$

where i is the iteration index, and $\Delta \varepsilon_j$, $j = 1, \cdots, 4$, is a small step size [36].

Although (27) and (32) give solutions to subchannel and power allocation, it is still necessary to design an executive algorithm. Consequently, we propose an optimal subchannel and power allocation (OSPA), shown in algorithm 1. ε_p is an arbitrarily small positive number. $\vartheta (i-1)$ and $\vartheta (i)$ are the variable values at the $(i-1)$ iteration and the i iteration. $\alpha_m (i)$, $\beta_m (i)$, $u_{nsk} (i)$ and $v_{ns} (i)$ are the Lagrangian multipliers at the i iteration. $\alpha_m (i+1)$, $\beta_m (i+1)$, $u_{nsk} (i+1)$ and $v_{ns} (i+1)$ are the Lagrangian multipliers at the $(i+1)$ iteration. In the OSPA, the computational complexity is in number of dual variables. Consequently, the computational complexity is given by $O \left(O_I M^2 \sum_{n \in \mathcal{N}} \sum_{s \in \mathcal{S}_n} \left| \mathcal{K}_{ns}^v \right| \right)$, where O_I is the number of iterations required for the convergence. Additionally, each secondary MT broadcasts its ρ_{nsm}^k and C_{nsm}^k to all serving secondary BSs, and the secondary BSs broadcast their $u_{nsk} (i+1)$, and $v_{ns} (i+1)$ to all secondary MTs. The total signal overhead is $O \left(\sum_{n \in \mathcal{N}} S_n + \sum_{n \in \mathcal{N}} \sum_{s \in \mathcal{S}_n} K_{ns}^v (1 + 2M_{ns}) \right)$.

Algorithm 1 Optimal Subchannel and Power Allocation (OSPA)

Require: E_m, τ, and I_{ns}^{th}.
Ensure: ρ_{nsm}^k, and C_{nsm}^k.
1: Initialize $\alpha_m (i) \geq 0$, $\beta_m (i) \geq 0$, $u_{nsk} (i) \geq 0$, $v_{ns} (i) \geq 0$, $\rho_{nsm}^k \geq 0$, $C_{nsm}^k \geq 0$, $i = 1$, and $\vartheta (i) = \min_{m \in \mathcal{M}} R_m$.
2: **repeat**
3:     Each secondary MT calculates ρ_{nsm}^k and C_{nsm}^k, and updates $\alpha_m (i+1)$ and $\beta_m (i+1)$.
4:     Each secondary BS updates $u_{nsk} (i+1)$, and $v_{ns} (i+1)$.
5:     **if** $\sum_{m \in \mathcal{M}_{ns}^c} \sum_{k \in \mathcal{K}_{ns}^v} C_{nsm}^k I_{nsm}^k \leq I_{ns}^{\text{th}}$, and $|\vartheta (i) - \vartheta (i-1)| \leq \varepsilon_p$ **then**
6:         Go to step 11;
7:     **else**
8:         Set $i \leftarrow i + 1$, and go to step 3;
9:     **end if**
10: **until**
11: Output ρ_{nsm}^k, and C_{nsm}^k.

B. Video Packet Scheduling

At each secondary MT, auction is a natural way in constructing economic model for video packet scheduling. Video packet auctioneer, who runs the auction, determines the winners, assigns the video packet, and charges the payments, exists a non-profit central entity for each secondary MT. At the beginning of each auction, each radio interface at secondary MT submits the total available transmission capacity to the spectrum auctioneer. If there is idle capacity available, each radio interface at secondary MT allows the video packet to transmit on it. On the other hand, secondary MT sends its private information, i.e., its video packets and its bidding price for each video packet. Based on these sealed-bid information, auctioneer performs the video packet scheduling, and calculates the payments and payoffs for each video packet at each radio interface. The auctioned capacity and the number of auctioned subchannels are defined by $\mathcal{CW}_m = \{CW_{nsm}\}$ and $\mathcal{BW}_m = \{BW_{nsm}\}$, where $CW_{nsm} = \sum_{k \in \mathcal{K}_{as}} R_{nsm}^k$ and BW_{nsm} are the capacity and the number of auctioned subchannels for cognitive network n BS s MT m, respectively. Only radio interfaces are bidders and the set of bid bundles is $\mathcal{B}_m = \{B_{nsm}\}$, $n \in \mathcal{N}$, $s \in \mathcal{S}_n$. Each bid B_{nsm} is specified as a 2-tuple (d_{nsm}, pv_{nsm}), where d_{nsm} is the capacity demand of each bidder, and pv_{nsm} is the amount that the bidder is willing to pay for d_{nsm}. For truthful auction, the bidding price equals the true valuation.

With $\mathcal{CW}_m$, $\mathcal{BW}_m$, and $\mathcal{B}_m$, the auctioneer formulates a video packet scheduling problem to determine how to maximize the video quality for each secondary MT, i.e.,

$$OP7: \max_{x_{nsm}^{fl}} V_m$$
$$s.t. \ (9) - (11), x_{nsm}^{fl} \in \{0, 1\} \quad (39)$$

Problem (39) is a binary integer programming, and a heuristic content-aware packet scheduling (CAPS) based on greedy algorithm is proposed in algorithm 2. rc_{nsm} is the remaining

Algorithm 2 Content-Aware Packet Scheduling (CAPS)

Require: CW_{nsm} and $l_f, \forall f \in \mathcal{F}$.
Ensure: x_{nsm}^{fl}.

1: Initialize $rc_{nsm} = C_{nsm}$, $\mathcal{A}$, $\mathcal{AV}$, x_{nsm}^{fl}, $r\left(l_f\right)$, and $\mathcal{B}_m$.
2: **repeat**
3:   Compute $\mathcal{AV} = \left\{ \mathcal{A}_i\left(1\right) v_f^{\mathcal{A}_i(1)} \right\}$, $\left(f^*, l^*\right) = \max\limits_{l_f \in \mathcal{L}_f, f \in \mathcal{F}} \mathcal{AV}$, and $\left(n^*, s^*\right) = \max\limits_{n \in \mathcal{N}, s \in \mathcal{S}_n} rc_{nsm}$.
4:   **if** $rc_{n^*s^*m} - r\left(l_{f^*}^*\right) \geq 0$ **then**
5:     Set $x_{n^*s^*m}^{f^*l^*} = 1$, and update $rc_{n^*s^*m} = C_{n^*s^*m} - r\left(l_{f^*}^*\right)$.
6:   **else**
7:     Set $x_{n^*s^*m}^{f^*l^*} = 0$, and drop this packet.
8:   **end if**
9:   **if** $\mathcal{A} \neq \emptyset$ **then**
10:     Delete the video packet, $\left(f^*, l^*\right)$, from $\mathcal{A}$, $\mathcal{AV}$, and $\mathcal{A}_i$, and go to step 3.
11:   **else**
12:     Stop and output x_{nsm}^{fl}.
13:   **end if**
14: **until**

capacity for cognitive network n BS s MT m, $\mathcal{A}_i$ is the ith group of video packets, $\mathcal{AV}$ is the distortion impact of video packets, and $\mathcal{A}$ is the set of the allocated video packets. The CAPS is implemented in each secondary MT. Additionally, the video packet auctioneer is each secondary MT, the bidders are the radio interfaces for its secondary MT, the sealed-bid information are its video packets and its bidding price for each video packet. Firstly, each secondary MT advertises video packets to different interfaces for auction, and classifies all video packets into AN groups, and the dependent video packets are classified into a group. Secondly, each secondary MT receives bids from different radio interfaces, and selects the first packet at each group into $\mathcal{A} = \{\mathcal{A}_i\left(1\right)\}$. Then, the secondary MT selects a video packet with the largest distortion impact, and picks up a radio interface with the largest remaining capacity. Finally, if the radio interface can afford the required transmission rate for the new assigned video packet, assign it; otherwise, drop this video packet. In the CAPS, the computational complexity is $O\left(\sum\limits_{n \in \mathcal{N}} \sum\limits_{s \in \mathcal{S}_n} 3N_{nsm}^P\right)$, where N_{nsm}^P is the number of allocated packets for cognitive network n BS s MT m. Additionally, each secondary MT broadcasts its information of video packets to all interfaces, and the overhead is $O\left(|\mathcal{A}|\right)$. The overhead of auction is $O\left(2|\mathcal{A}||\mathcal{N}|\right)$. The total signal overhead is $O\left(\left(2|\mathcal{N}| + 1\right)|\mathcal{A}|\right)$.

V. PERFORMANCE EVALUATION

The simulation results is presented for proposed algorithms to solve joint video packet scheduling, subchannel assignment and power allocation problem. There is a geographical region, covered by one cognitive macrocell and one cognitive microcell. The radius of each cognitive macrocell is 400 m, while the radius of each cognitive microcell is 200 m. Due to the overlapped coverage between cognitive macrocell and
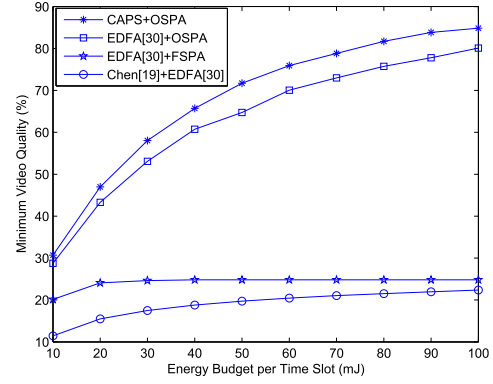

Fig. 3. Minimum video quality versus energy budget per time slot.

cognitive microcell, two service areas exist and secondary MTs get service from both cognitive macrocell BS and cognitive microcell BS. The path loss exponent is 4, and the amplitude of multipath fading is Rayleigh. The noise power is 5×10^{-19} W/Hz. The number of subcarriers for each macrocell and each microcell are both 64. The busy probability of each subcarrier is 0.5, and the vacant probability of each subcarrier is also 0.5. The other simulation parameters are $\eta_{nsm} = 0.35$, $Q_{nsm} = 1$ mW, $\tau = 400$ ms, $\Delta D = 40$ ms, and $\zeta_{nsm} = 20 \times 10^{-9}$ W/Hz. Video sequences are compressed with an MPEG4-FGS encoder, at 30 fps with the GoP structure [37]. Additionally, the GoP structure includes 12 frames from one layer. Specifically, the frame lengths for I, B and P frames are 9600 bits, 8000 bits, and 6000 bits, respectively. Additionally, each I frame has 12 packets, and each of B and P frames have both 10 packets. Consequently, each video packet in I and P frames requires transmission rate 8 Kbps, while that in B frame needs transmission rate 6 Kbps. The packet distortion impact values for I, P, and B frames are $v_f^l = 5$, $v_f^l = 4$, and $v_f^l = 2$, respectively [3]. Compared with CAPS+OSPA, the benchmark is an earliest deadline first approach (EDFA) [34], and a fixed subchannel and power allocation (FSPA) is adopted. Additionally, we compare our proposed algorithms with Chen's algorithm in [20], which is designed resource allocation based on multi-homing technology for heterogeneous cognitive radio networks. However, Chen's algorithm does not consider the video packet scheduling algorithm. Hence, the video packet scheduling adopts the EDFA for Chen's algorithm.

We evaluate the impact of the energy budget per time slot on minimum video quality in Fig. 3. The number of secondary MTs in each cell is $M_{ns} = 5$. The available bandwidth for each subcarrier is 0.0781 MHz. The interference power threshold is $I_{ns}^{\text{th}} = 5 \times 10^{-11}$ W. The secondary MT available energy is 180 Joule. From Fig. 3, we observe that CAPS+OSPA has the largest minimum video quality. This is because CAPS+OSPA not only increases the available transmission rate for each secondary MT at the physical layer, but also obtains the content-aware scheduling gain. Additionally, the minimum video quality for four algorithms increase with the energy budget per time slot, which can be explained that increasing energy budget per time slot can increase the available power at each secondary MT, and further enhance the total number of scheduled video packets.
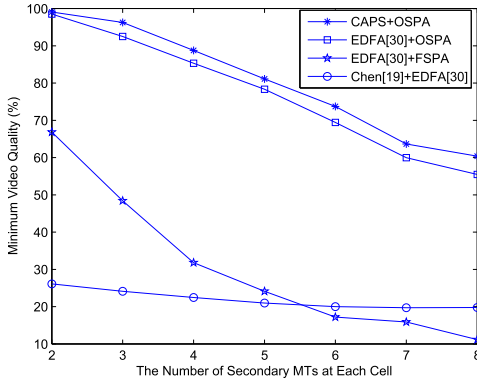
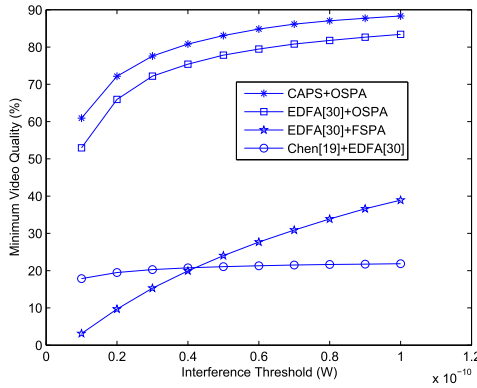Fig. 4. Minimum video quality versus the number of secondary MTs at each cell.

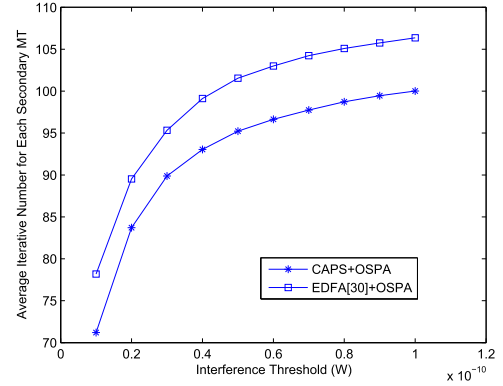Fig. 5. Minimum video quality versus interference threshold.

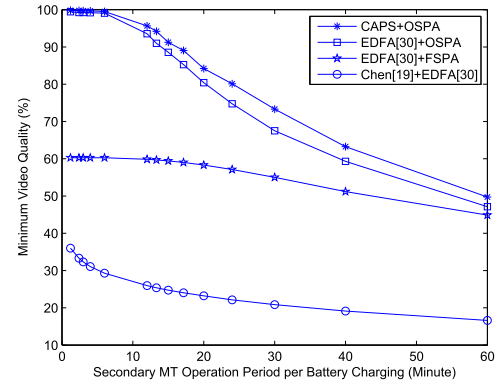Fig. 6. Average iterative number of video packet scheduling for each secondary MT versus interference threshold.

Fig. 7. Minimum video quality versus secondary MT operation period per battery charging.

We evaluate the impact of the number of secondary MTs at each cell on minimum video quality in Fig. 4. The available bandwidth for each subcarrier is 0.0781 MHz. The interference power threshold is $I_{ns}^{th} = 5 \times 10^{-11}$ W. The energy budget, E_m, per time slot is 80 mJ. The secondary MT available energy is 180 Joule. It can be observed that the minimum video quality for four algorithms decrease along with the number of secondary MTs at each cell. This is because increasing the number of secondary MTs leads to the fact that the available subchannel resource for each secondary MT decreases, and each secondary MT will consume more energy to guarantee the video quality. It can also see that the minimum video quality for EDFA+OSPA is smaller than that of CAPS+OSPA. The reason is that, in EDFA, video packets are scheduled earlier, and CAPS is a content-aware scheduling algorithm. Consequently, CAPS obtains the video scheduling gain in the time domain, and improves the minimum video quality further.

We evaluate the impact of the interference power threshold on minimum video quality and the average iterative number of the video packet scheduling for each secondary MT in Fig. 5 and Fig. 6. The available bandwidth for each subcarrier is 0.0781 MHz. The energy budget, E_m, per time slot is 80 mJ. The number of secondary MTs in each cell is $M_{ns} = 5$. The secondary MT available energy is 180 Joule. In Fig. 5, it can be observed that the minimum video quality for four algorithms grows with the interference power threshold. Since increasing the interference power threshold not only results in the growth of the capacity region in cognitive heterogeneous networks,

but also increases the available power consumption for each radio interference at each secondary MT. It can also see that the minimum video quality for Chen+EDFA is smaller than that of EDFA+OSPA. The reason is that Chen's algorithm allocates the subchannel and power without considering the video packet scheduling and video quality at the link layer. In Fig. 6, we can see that the average iterative number of video packet scheduling for CAPS+OSPA is smaller than that for EDFA+OSPA. Hence, we can conclude that CAPS+OSPA not only achieves the higher minimum video quality, but also has more efficiency to schedule the video packet.

We evaluate the impact of secondary MT operation period per battery charging on minimum video quality in Fig. 7. The available bandwidth for each subcarrier is 0.0938 MHz. The number of secondary MTs in each cell is $M_{ns} = 5$. The interference power threshold is $I_{ns}^{th} = 2 \times 10^{-10}$ W. The secondary MT available energy is 180 Joule. From Fig. 7, we can see that the minimum video quality for four algorithms decrease along with secondary MT operation period per battery charging. The reason is that the more secondary MT operation period per battery charging is, the less the available energy budget per time slot is. Additionally, the gap between EDFA+OSPA and Chen+EDFA is larger than that between EDFA+OSPA and CAPS+OSPA, which can be explained that the video quality improved gain obtained by the subchannel and power allocation exceeds that with the video packet scheduling.

We evaluate the fairness of video quality among different secondary MTs in Fig. 8. The number of secondary MTs
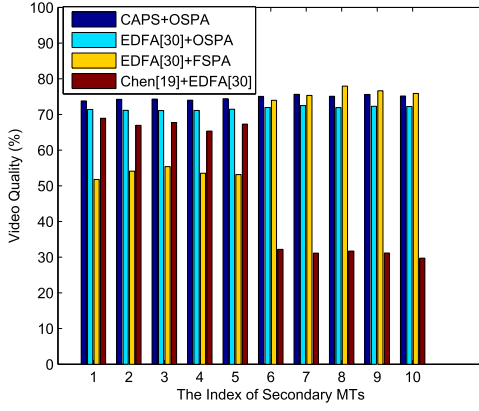
Fig. 8. Minimum video quality versus the index of secondary MTs.

in each cell is $M_{ns} = 5$. The available bandwidth for each subcarrier is 0.0781 MHz. The interference power threshold is $I_{ns}^{th} = 4 \times 10^{-11}$ W. The secondary MT available energy is 180 Joule. The energy budget, E_m, per time slot is 60 mJ. From Fig. 8, we can see that CAPS+OSPA and EDFA+OSPA can achieve the better video quality fairness than EDFA+FSPA and Chen+EDFA. This is due to the fact that OSPA jointly allocates the subchannel and power to guarantee the available transmission rate fairness for secondary MTs, which can improve the video quality fairness among different secondary MTs. Although EDFA+OSPA can also achieve the good video quality fairness, its video quality is smaller than that of CAPS+OSPA. From Fig. 3 to Fig. 8, it can be concluded that CAPS+OSPA not only improves the minimum video quality for cognitive heterogeneous networks significantly, but also guarantees the video quality fairness among different secondary MTs.

VI. Conclusion

In this work, content-aware video transmission scheme is investigated for cognitive heterogeneous networks. The optimization objective maximizes the minimum video quality for different secondary MTs with the joint subchannel and power allocation and video packet scheduling. Additionally, the joint physical layer and link layer resource allocation problem is modeled as MINLP and is divided into two sub-problems. In the first sub-problem, the joint subchannel and power allocation is formulated as a max-min fractional programming, given the total available subchannels, CSI, the total allowed interference power, and the secondary MT's energy. In order to solve it, the dual decomposition method is utilized to design an optimal subchannel and power allocation algorithm. In the second sub-problem, video packets for each secondary MT are allocated among different radio interfaces to maximize the video quality. Additionally, the video packet scheduling problem is mapped as a forward-auction problem, and a heuristic video packet scheduling scheme is proposed. Numerical results demonstrate that the proposed framework improves the video transmission quality significantly.

Appendix
Proof of Proposition 1

Proof. Since the objective function, $U(\vartheta) = \log_2(1 + \vartheta)$, is a convex function, we fucus on proving the constraints to

constitute a convex set on ρ_{nsm}^k and C_{nsm}^k. Firstly, we prove the convexity for the first constraint in (16). Set the second derivative R_m on ρ_{nsm}^k and C_{nsm}^k is

$$\frac{\partial^2 R_m}{\partial \left(\rho_{nsm}^k\right)^2} = -\frac{\Pr_{ns}^{2,k} B_{ns} \left(C_{nsm}^k g_{nsm}^k\right)^2}{\rho_{nsm}^k \left[W_{nsm}^k\right]^2 \ln 2} \le 0 \qquad (40)$$

and

$$\frac{\partial^2 R_m}{\partial \left(C_{nsm}^k\right)^2} = -\frac{\Pr_{ns}^{2,k} B_{ns} \left(g_{nsm}^k\right)^2 \rho_{nsm}^k}{\left(W_{nsm}^k\right)^2 \ln 2} \le 0. \qquad (41)$$

From (40) and (41), R_m is convex on both ρ_{nsm}^k and C_{nsm}^k. Additionally, it is easily to prove the convexities of the other constraints.

References

[1] D. I. Kim, E.-H. Shin, and M. S. Jin, "Hierarchical power control with interference allowance for uplink transmission in two-tier heterogeneous networks," *IEEE Trans. Wireless Commun.*, vol. 14, no. 2, pp. 616–627, Feb. 2015.

[2] S. A. Ahmad and D. Datla, "Distributed power allocations in heterogeneous networks with dual connectivity using backhaul state information," *IEEE Trans. Wireless Commun.*, vol. 14, no. 8, pp. 4574–4581, Aug. 2015.

[3] M. Ismail and W. Zhuang, "Mobile terminal energy management for sustainable multi-homing video transmission," *IEEE Trans. Wireless Commun.*, vol. 13, no. 8, pp. 4616–4627, Aug. 2014.

[4] H. Boostanimehr and V. K. Bhargava, "Unified and distributed QoS-driven cell association algorithms in heterogeneous networks," *IEEE Trans. Wireless Commun.*, vol. 14, no. 3, pp. 1650–1662, Mar. 2015.

[5] S. Mallick, R. Devarajan, R. A. Loodaricheh, and V. K. Bhargava, "Robust resource optimization for cooperative cognitive radio networks with imperfect CSI," *IEEE Trans. Wireless Commun.*, vol. 14, no. 2, pp. 907–920, Feb. 2015.

[6] C. Ghosh, S. Roy, and D. Cavalcanti, "Coexistence challenges for heterogeneous cognitive wireless networks in TV white spaces," *IEEE Wireless Commun.*, vol. 18, no. 4, pp. 22–31, Aug. 2011.

[7] M. Siekkinen, M. A. Hoque, and J. K. Nurminen, "Using viewing statistics to control energy and traffic overhead in mobile video streaming," *IEEE/ACM Trans. Netw.*, vol. 24, no. 3, pp. 1489–1503, Jun. 2016.

[8] Q. M. Qadir, A. A. Kist, and Z. Zhang, "A novel traffic rate measurement algorithm for quality of experience-aware video admission control," *IEEE Trans. Multimedia*, vol. 17, no. 5, pp. 711–722, May 2015.

[9] S.-Y. Lien and S.-M. Cheng, "Performance guaranteed statistical traffic control in cognitive cellular networks," in *Proc. IEEE WPMC*, Jun. 2013, pp. 1–5.

[10] H.-P. Shiang and M. van der Schaar, "Dynamic channel selection for multi-user video streaming over cognitive radio networks," in *Proc. IEEE ICIP*, Oct. 2008, pp. 2316–2319.

[11] S.-Y. Lien and K.-C. Chen, "Statistical traffic control for cognitive radio empowered LTE-advanced with network MIMO," in *Proc. IEEE INFOCOM WKSHPS*, Apr. 2011, pp. 80–84.

[12] H. Saki and M. Shikh-Bahaei, "Cross-layer resource allocation for video streaming over OFDMA cognitive radio networks," *IEEE Trans. Multimedia*, vol. 17, no. 3, pp. 333–345, Mar. 2015.

[13] B. Guan and Y. He, "Optimal resource allocation for video streaming over cognitive radio networks," in *Proc. IEEE MMSP*, Oct. 2011, pp. 1–6.

[14] B. Guan and Y. He,, "Optimal resource allocation for multi-layered video streaming over multi-channel cognitive radio networks," in *Proc. IEEE TrustCom*, Jun. 2012, pp. 1525–1528.

[15] D. Hu and S. Mao, "Resource allocation for medium grain scalable videos over femtocell cognitive radio networks," in *Proc. IEEE ICDCS*, Jun. 2011, pp. 258–267.

[16] L. Zhou, R. Q. Hu, Y. Qian, and H.-H. Chen, "Energy-spectrum efficiency tradeoff for video streaming over mobile ad hoc networks," *IEEE J. Sel. Areas Commun.*, vol. 31, no. 5, pp. 981–991, May 2013.

[17] L. Zhou, Z. Yang, Y. Wen, and J. J. P. C. Rodrigues, "Distributed wireless video scheduling with delayed control information," *IEEE Trans. Circuits Syst. Video Technol.*, vol. 24, no. 5, pp. 889–901, May 2014.

[18] A. Bhattacharya, R. Ghosh, K. Sinha, D. Datta, and B. P. Sinha. (Mar. 2016). "Multimedia channel allocation in cognitive radio networks using FDM-FDMA and OFDM-FDMA." [Onlilne]. Available: https://arxiv.org/abs/1603.03938

[19] M. H. Yilmaz, M. M. Abdallah, H. M. El-Sallabi, J. F. Chamberland, K. A. Qaraqe, and H. Arslan, "Joint subcarrier and antenna state selection for cognitive heterogeneous networks with reconfigurable antennas," *IEEE Trans. Commun.*, vol. 63, no. 11, pp. 4015–4025, Nov. 2015.

[20] F. Chen, W. Xu, Y. Guo, J. Lin, and M. Chen, "Resource allocation in OFDM-based heterogeneous cognitive radio networks with imperfect spectrum sensing and guaranteed QoS," in *Proc. IEEE CHINACOM*, Aug. 2013, pp. 46–51.

[21] R. Xie, F. R. Yu, H. Ji, and Y. Li, "Energy-efficient resource allocation for heterogeneous cognitive radio networks with femtocells," *IEEE Trans. Wireless Commun.*, vol. 11, no. 11, pp. 3910–3920, Nov. 2012.

[22] L. Fu, X. Wang, and P. R. Kumar, "Are we connected? Optimal determination of source-destination connectivity in random networks," *IEEE/ACM Trans. Netw.*, to be published.

[23] M. Ismail, A. T. Gamage, W. Zhuang, X. Shen, E. Serpedin, and K. Qaraqe, "Uplink decentralized joint bandwidth and power allocation for energy-efficient operation in a heterogeneous wireless medium," *IEEE Trans. Commun.*, vol. 63, no. 4, pp. 1483–1495, Apr. 2015.

[24] M. Ismail, W. Zhuang, and S. Elhedhli, "Energy and content aware multi-homing video transmission in heterogeneous networks," *IEEE Trans. Wireless Commun.*, vol. 12, no. 7, pp. 3600–3610, Jul. 2013.

[25] U. Tefek and T. J. Lim, "Interference management through exclusion zones in two-tier cognitive networks," *IEEE Trans. Wireless Commun.*, vol. 15, no. 3, pp. 2292–2302, Mar. 2016.

[26] M. Levorato, U. Mitra, and M. Zorzi, "Cognitive interference management in retransmission-based wireless networks," *IEEE Trans. Inf. Theory*, vol. 58, no. 5, pp. 3023–3046, May 2012.

[27] C. Yi and J. Cai, "Combinatorial spectrum auction with multiple heterogeneous sellers in cognitive radio networks," in *Proc. IEEE ICC*, Jun. 2014, pp. 1626–1631.

[28] G. Lim and L. J. Cimini, "Energy-efficient cooperative relaying in heterogeneous radio access networks," *IEEE Wireless Commun. Lett.*, vol. 1, no. 5, pp. 476–479, Oct. 2012.

[29] Y. Zhang and C. Leung, "Resource allocation in an OFDM-based cognitive radio system," *IEEE Trans. Commun.*, vol. 57, no. 7, pp. 1928–1931, Jul. 2009.

[30] S. Wang, M. Ge, and W. Zhao, "Energy-efficient resource allocation for OFDM-based cognitive radio networks," *IEEE Trans. Commun.*, vol. 61, no. 8, pp. 3181–3191, Aug. 2013.

[31] M. K. Afzal, B.-S. Kim, and S. W. Kim, "Efficient and reliable MPEG-4 multicast MAC protocol for wireless networks," *IEEE Trans. Veh. Tech.*, vol. 64, no. 3, pp. 1026–1035, Mar. 2015.

[32] Z. Pan, Y. Zhang, and S. Kwong, "Efficient motion and disparity estimation optimization for low complexity multiview video coding," *IEEE Trans. Broadcast.*, vol. 61, no. 2, pp. 166–176, Jun. 2015.

[33] Z. Pan, J. Lei, Y. Zhang, X. Sun, and S. Kwong, "Fast motion estimation based on content property for low-complexity H.265/HEVC encoder," *IEEE Trans. Broadcast.*, vol. 62, no. 3, pp. 675–684, Sep. 2016.

[34] D. Jurca and P. Frossard, "Video packet selection and scheduling for multipath streaming," *IEEE Trans. Multimedia*, vol. 9, no. 3, pp. 629–641, Apr. 2007.

[35] Q. Xu, X. Li, H. Ji, and X. Du, "Energy-efficient resource allocation for heterogeneous services in OFDMA downlink networks: Systematic perspective," *IEEE Trans. Veh. Technol.*, vol. 63, no. 5, pp. 2071–2082, Jun. 2014.

[36] S. Boyd and L. Vandenberghe, *Convex Optimization*. Cambridge, U.K.: Cambridge Univ. Press, 2004.

[37] H. M. Radha, M. V. D. Schaar, and Y. Chen, "The MPEG-4 fine-grained scalable video coding method for multimedia streaming over IP," *IEEE Trans. Multimedia*, vol. 3, no. 1, pp. 53–68, Mar. 2001.

Lei Xu (M'16) received the bachelor's, master's, and Ph.D. degrees in communication and information systems from the Nanjing University of Aeronautics and Astronautics, China, in 2006, 2009, and 2012, respectively. He is currently an Associate Professor with the School of Computer Science and Engineering, Nanjing University of Science and Technology, Nanjing, China. His research interests include 5G wireless network, network analysis, Internet of Things, satellite communication, and radar signal processing.

Arumugam Nallanathan (S'97–M'00–SM'05–F'17) was an Assistant Professor with the Department of Electrical and Computer Engineering, National University of Singapore, from 2000 to 2007.

He served as the Head of Graduate Studies with the Faculty of Natural and Mathematical Sciences, King's College London (University of London), from 2011 to 2012, where he is currently a Professor of Wireless Communications with the Department of Informatics. His current research interests include 5G wireless networks, Internet of Things, and molecular communications.

He is a co-recipient of the Best Paper Awards presented at the IEEE International Conference on Communications 2016 (ICC'2016) and the IEEE International Conference on Ultra-Wideband 2007 (ICUWB2007). He has been selected as a Web of Science (ISI) Highly Cited Researcher (also known as the World's Most Influential Scientific Minds) in 2016. He is an IEEE Distinguished Lecturer. He is an Editor of the IEEE TRANSACTIONS ON COMMUNICATIONS and the IEEE TRANSACTIONS ON VEHICULAR TECHNOLOGY, and a Guest Editor of the IEEE TRANSACTIONS ON EMERGING TOPICS IN COMPUTING: SPECIAL ISSUE ON ADVANCES IN MOBILE AND CLOUD COMPUTING. He was an Editor of the IEEE TRANSACTIONS ON WIRELESS COMMUNICATIONS (2006–2011), the IEEE WIRELESS COMMUNICATIONS LETTERS and the IEEE SIGNAL PROCESSING LETTERS. He served as the Chair for the Signal Processing and Communication Electronics Technical Committee of IEEE Communications Society, Technical Program Co-Chair (MAC track) of the IEEE WCNC 2014, Co-Chair of the IEEE GLOBECOM 2013 (Communications Theory Symposium), Co-Chair of the IEEE ICC 2012 (Signal Processing for Communications Symposium), Co-Chair of the IEEE GLOBECOM 2011 (Signal Processing for Communications Symposium), Technical Program Co-Chair of the IEEE International Conference on UWB 2011 (IEEE ICUWB 2011), Co-Chair of the IEEE ICC 2009 (Wireless Communications Symposium), Co-Chair of the IEEE GLOBECOM 2008 (Signal Processing for Communications Symposium), and General Track Chair of the IEEE VTC 2008. He received the IEEE Communications Society Signal Processing and Communications Electronics Outstanding Service Award 2012 and the IEEE Communications Society RCC Outstanding Service Award 2014.

Xiaoqin Song photograph and biography not available at the time of publication.